



OPEN Green synthesis of iron and zinc nanoparticles, total phenolic and total flavonoid components, and pharmacological studies of *Perovskia atriplicifolia* Benth

Amjad Hussain¹✉, Ahmad Bilal¹, Sajjad Azam¹, Muhammad Sajid Hamid Akash², Muhammad Imran³, Enas Ali⁴, Katarzyna Kotwica-Mojzych⁵, Mariola Glowacka⁶, Mariusz Mojzych⁶, Meher Ali⁷, Muhammad Adnan Ayub⁸, Khayala Mammadova⁹, Afnan Jan¹⁰ & Ajmal Khan^{11,12}

Perovskia atriplicifolia Benth. commonly known as Russian sage, is an important ornamental and medicinal plant native to Himalayas and western China. In traditional medicine, it has been used in the treatment of various diseases such as stomach pain, indigestion, fever, dysentery and in various bacterial infections. This study investigated the green synthesis of iron and zinc nanoparticles, phytochemicals, and biological evaluation of *P. atriplicifolia* with emphasis on its therapeutic potentials. The characterization of nanoparticles was performed through SEM, XRD, FT-IR and UV. The activities, including cytotoxicity, thrombolytic, antibacterial, and anti-inflammatory, were conducted on the different polarity extracts of *P. atriplicifolia* and nanoparticles. Among all, ethyl acetate extract (PAE), dichloromethane extract (PAD), and Zn-NPs were shown to have significant results. Total phenolic content (TPC) and total flavonoid content (TFC) in the crude extract were 258.96 mg GAE/g and 511.71 mg CE/g, respectively. In vitro studies have shown that *P. atriplicifolia* possesses significant biological potentials that encourage its traditional medicinal uses. Based on these findings, it can be exploited in the development of various therapeutic products. However, there is a dire need for systematic examination in clinical trials to determine the safe dosage and efficacy of *P. atriplicifolia* for the treatment of several disorders.

Keywords Phytochemistry, Green synthesis, Cytotoxicity, Antibacterial, Anti-thrombolytic, Anti-inflammatory

Abbreviations

| | |
|------|--|
| FTIR | Fourier transform infra-red spectroscopy |
| UV | Ultra-violet spectroscopy |
| SEM | Scanning electron microscope |

¹Department of Chemistry, University of Okara, Okara 56300, Pakistan. ²Department of Pharmaceutical Chemistry, Government College University, Faisalabad, Pakistan. ³Central Labs, Department of chemistry, Faculty of Science, King Khalid University, AlQura'a, P.O. Box 960, Abha 61413, Saudi Arabia. ⁴Centre for Research Impact & Outcome, Chitkara University Institute of Engineering and Technology, Chitkara University, Rajpura, Punjab 140401, India. ⁵Department of Histology, Embriology and Cytophysiology, Medical University of Lublin, Radziwillowska 11, Lublin 20-080, Poland. ⁶Faculty of Human Science Collegium Medicum, The Mazovian Academy in Plock, Pl. Dabrowskiego 2, Plock 09-402, Poland. ⁷Department of Chemistry, Karakoram International University, Gilgit 15100, Pakistan. ⁸Department of Chemistry, University of Sahiwal, Sahiwal, Punjab 57000, Pakistan. ⁹Medical and Biological Physics Department, Azerbaijan Medical University, Baku, Azerbaijan. ¹⁰Department of Biochemistry, Faculty of Medicine, Umm Al-Qura University, Makkah, Kingdom of Saudi Arabia. ¹¹Natural and Medical Sciences Research Center, University of Nizwa, Birkat Al Mauz, P.O. Box 33, Nizwa 616, Sultanate of Oman. ¹²Department of Chemical and Biological Engineering, College of Engineering, Korea University, 145 Anam-ro, Seongbuk-gu, Seoul 02841, Republic of Korea. ✉email: amjadhussain@uo.edu.pk

| | |
|-------|-----------------------------------|
| XRD | X-ray diffraction |
| TPC | Total phenolic content |
| TFC | Total flavonoid content |
| PAE | Ethyl acetate extract |
| PAD | Dichloromethane extract |
| PAH | n-Hexane extract |
| PAB | n-Butane extract |
| NPs | Nano-particles |
| DMF | Dimethyl formamide |
| ELISA | Enzyme-linked immunosorbent assay |
| MIC | Minimum inhibitory concentration |
| PBS | Phosphate buffered saline |
| RBCs | Red blood cells |

Nanoparticles are particles with one or more dimensions that range in size from 1 nm to 100 nm, according to ISO and ASTM standards. In the nano metric scale, nanoparticles are divided into organic, inorganic, and carbon-based particles, which have better qualities than bigger sizes of respective materials. Because of their small size, nanoparticles have increased qualities such as strong reactivity, strength, surface area, sensitivity and stability¹. Nanoparticles are made for research and commercial applications utilizing a range of technologies classified into three categories: physical, chemical, and mechanical procedures, all of which have significantly improved over time. Modern research emphasized on nanoparticles, including their varieties, properties, synthesis methods, and applications in the environment. The nanoparticles prepared by biological components are called biogenic nanoparticles. The process used for the preparation of biogenic nanoparticles is known as green synthesis^{2,3}. The importance of this method is due to its less energy consumption and no use of any toxic chemicals. For biosynthesis, micro-organisms and plants extract are used. Nanoparticles are characterized by using different techniques such as FTIR (Fourier transform infra-red spectroscopy), UV (Ultra-violet spectroscopy), SEM (Scanning electron microscope) and XRD (X-ray diffraction)^{4,5}.

Perovskia atriplicifolia benth., is a plant that grows in bushes mostly found in the areas of Pakistan, Iran and Afghanistan^{6,7}. There are seven species in the *Perovskia* genus, which belong to the *Labiatae* family⁸. Only three species of *Perovskia* have been studied for phytochemical and pharmacological activities in the south Asian and central Asian countries. Sefldkon et al. (1997) extracted essential oil from the aerial part of *P. atriplicifolia* and observed that, mostly compounds were terpenes⁹. Jassbi et al. (1999) performed hydro distillation of its aerial part and identified 19 compounds which were monoterpenes and sesquiterpenes¹⁰. Ali et al. (2001) isolated acylated steroid glucoside from this plant¹¹. Pourmortazavi et al. (2003) performed SFE and steam distillation extraction of its aerial part and observed that at higher temperature, the components ratio was reduced in it and with low pressure, the constituent's ratio was increased in these extracts¹². Perveen et al. (2005) purified four compounds from the ethyl acetate extract of this plant and observed that first compound; Perovskoate shown inhibition against lipoxygenase and cholinesterase⁵. They also isolated pervosides A-B, two novel compounds from the same extract in another study¹³. In similar study, they isolated the new triterpenoidal and flavonone glucosides A-B from the ethyl acetate extract¹⁴. Erdemgil et al. (2008) studied the phytochemistry of its essential oil and identified 18 different class of compounds in it. They also evaluated the antimicrobial activity of extracted essential oil against 10 bacterial strains and 5 fungal strains with ager diffusion method. The results have been shown the potential in antimicrobial and antimutagenic activity of essential oil¹⁵. Jiang et al. (2013) extracted new perovskatone A triterpene with 9 known compounds. In-vitro anti-HBV assays showed that this new compound have potent inhibitory action on hepatitis B¹⁶. Perveen et al. (2014) isolated erythrodiol, β -amyrin, oleanolic acid, glycyrrhetic acid, 2a,3b-dihydroxyolean-12-en-28-methyl ester, 3 β -hydroxy-11,13(18)-oleanadien-28-oic acid, 2a,3b,24-trihydroxyolean-12-en-28-oic acid, 2a,3b-dihydroxyolean-12-en-28-oic acid and 2a,3b,19b-trihydroxyurs-12-en-28-oic acid from *P. atriplicifolia* and evaluated its potential against the inhibition of butyrylcholinesterase, showing potent results¹⁷. Jiang et al. (2014) isolated eight compounds from *P. atriplicifolia*, All compounds were evaluated in anti-HBV activity and find that these compounds have inhibitory action on HBsAg and HBeAg secretion¹⁸. Jiang et al. (2015) purified 5 new icetexane diterpenoids and 2 known compounds, i.e., perzewalskin E and brussionol which were assessed against anti-hepatitis B virus, results shown the potential behavior of these compounds¹⁹. Slusarczyk et al. (2015) isolated eight nor-abietanoid from the roots of *P. atriplicifolia*²⁰. Miroliaei et al. (2017) evaluated the extract of *P. atriplicifolia* in inhibition of glycation of albumin and also working in the controlling of cell damage in four mammalian cell lines. Its extract has shown considerable results in inhibition of glycated albumin toxicity and cell survival by 50%. These results have shown the antiglycative and antiglycotoxic potential of *P. atriplicifolia* extract²¹. Liu et al. (2018) isolated two new terpenoids namely, biperovskatone B and 1- α hydroxyl demethylsalvicanol quinone from the culture of *P. atriplicifolia* and found their anti-HBV activity with IC₅₀ 10.78 and 8.61 μ M values²². Slusarczyk et al. (2020) isolated three new compounds (1R,15R)-1-acetoxycryptotanshinone, (1R)-1-acetoxytanshinone IIA, and (15R)-1-oxoaegyptinone A and isograndifoliol and evaluated against colinesterase and butyrylacetylcolinesterase activity. Molecular docking and in silico toxicology studies showed the active behavior in these disorders²³.

P. atriplicifolia is a decorative shrub known for its attractive flowers and pleasant fragrance. While several studies have focused on the phytochemical composition of its essential oils, there is a lack of published data regarding its antibacterial, cytotoxic, and anti-thrombolytic activities, particularly from its different polarity plant extracts. The present study aims to provide scientific validation of these pharmacological properties in relation to the plant's traditional medicinal uses. Additionally, we conducted a comparative phytopharmacological evaluation of the crude plant extracts and their corresponding Fe and Zn nanoparticles synthesized via a green

approach. Nanoparticle formation is known to enhance the bioavailability and biological activity of plant-derived compounds. To our knowledge, this is the first study to synthesize and assess Fe and Zn nanoparticles from *P. atriplicifolia*, thereby uncovering its untapped pharmacological potential and expanding its application in nanomedicine.

Materials and methods

Plant collection

Perovskia atriplicifolia was collected from Parachinar, Khyber Pakhtunkhwa, Pakistan (33°90'N, 70°09'E) in the month of August. This plant was identified by Botanist, Dr. Faheem Arshad, Associate Professor/Chairperson, Department of Botany, University of Okara, Okara, Pakistan. The plant specimen was submitted to the Herbarium of Department of Botany, University of Okara with **Voucher Specimen Number # UO-H-BOT-55**. The collected plant was dried in the shaded area. After that, the dried plant was crushed into fine powdered form.

Preparation of *P. atriplicifolia* fractions

The dried mass of plant was soaked in 95% methanol (3 × 7 d). After this, the methanol was filtered and evaporated in rotary evaporator. The obtained crude extract was subjected into solvent extraction technique with gradient polarity solvents to get n-hexane (PAH), dichloromethane (PAD), ethyl acetate (PAE), n-butanol (PAB) and aqueous extracts (PAA)^{1,24}.

Green synthesis

Preparation of stock solution

To synthesize nanoparticles, 0.01 M stock solutions of ZnCl₂ and FeCl₃·6H₂O were prepared in distilled water. These substances were all purchased from Sigma-Aldrich.

Biosynthesis of nanoparticles

To get the green synthesized iron nanoparticles, we took 0.5 ml crude extract of *P. atriplicifolia* in 45 ml of distilled water. Prepared its homogeneous solution and then filtered it. After this, we took 1 mM FeCl₃·6H₂O salt in beaker, containing 5 ml distilled water. Both the solutions were mixed and heated on 70 °C for 60 min. Then the solution placed to get its temperature normal. After 24 h, the precipitations were made in the solution. These mixtures were then filtered by centrifuge machine CNWTC-(80 – 2/4000 RPM). The obtained precipitate/nanoparticles were washed with distilled water. These precipitates were used for further experimentations. Similarly, Zn nanoparticles were obtained by mixing 5 ml of 1 mM ZnCl₂ salt solution in distilled water with 45 ml of crude extract solution (0.5 ml/45 ml distilled water). The solution was heated on 70 °C for 1 h, then placed to settle down its precipitates for the 24 h. The precipitates/nanoparticles were collected after centrifugation and washed with distilled water for characterization¹.

SEM analysis

The most stable nanoparticles are considered to be the best candidates when analyzing them physically. The SEM images were obtained for the determining the surface morphology of the prepared nanoparticles from the machine (SEM) (JEOL, JSM-6400, Japan) with a secondary electron detector at an accelerating voltage of 15 kV. For the determination of sizes of newly prepared nanoparticles, ImageJ (ImageJ version 1.54 h) (<https://imagej.nih.gov/ij/download.html>) software was used.

UV analysis

A BK-D560 spectrophotometer (China) has been used to record UV visible spectra at room temperature in order to evaluate the green synthesis and stability of nanoparticles. The methanol solution was used to draw the baseline, and a wave length (λ) ranging from 200 nm to 600 nm was used. The green synthesis of iron and zinc nanoparticles were assessed by the peaks at 270–320 nm and 310–350 nm, respectively.

X-ray diffraction analysis

Green synthesized iron and zinc nanoparticles were scanned through Philips-XPert Pro MPD (Netherlands) XRD machine with MG, in which radioactive source was high power Cu-Kα with 0.154 nm λ at 40 kV/40 mA. Scanning rate was 3° 2θ per minute from 10° to 80° 2θ. This range mostly covered all species of iron, zinc and their oxides.

FT-IR analysis

To get the FT-IR analysis of this plant crude extract, iron and zinc nanoparticles, IR Spirit with QATR-S Mounted (a single-reflection ATR accessory with a diamond crystal) was used.

Determination of total phenolic components

According to Julkenen-Titto assay, the phenolic components of crude extract of subjected plant species were determined. In this experiment, a test tube was filled with 100 μL of crude extract (1 mg/ml) along with 1 ml of Folin-Ciocalteu reagent. After that, the final volume was raised to 10 ml with distilled water. The mixture in test tube was vortexed at room temperature, followed by incubation for 5 min. Take 2 ml of NaCO₃ (7.5%) in it and then placed the test tube mixture in the dark for 120 min. The absorbance of sample was observed at 765 nm by using spectrophotometer (Lambda 25, PerkinElmer USA). Gallic acid was used as reference in this assay, which had 0.99 R² value²⁵.

Determination of total flavonoids components

The flavonoid component of the crude extract was determined using an aluminum chloride colorimeter test. Sample and reference (catechin) were prepared in 20, 40, 60–100 mg/L concentrations. Take 1 ml of these preparations in 10 ml flask separately, then add 4 ml distilled water in it. The next step was to add 300 μ L of 5% sodium nitrite. The mixture was placed for 10 min and then add 300 μ L of 10% aluminium chloride in the mixture. 2 mL of sodium hydroxide (1 M) were added into the flask after a minute, and distilled water was used to raise the volume to ten milliliters. After that, the entire solution was shaken and exposed to UV light in order to quantify the absorbance at 510 nm. TFC in the crude extract was determined in milligrams of catechin equivalents (mg CE) per gram, with an R2 value of 0.9835²⁶.

In vitro biological assays

Evaluation of cytotoxicity

After carefully mixing 3 mL of human blood, they were placed in a five-milliliter sterile polystyrene screw cap tube weighing 80 g, and they were centrifuged for five minutes. After the surplus was drained off, the sticky product was rinsed three times with cooled sterile isotonic phosphate buffered saline solution. A hemocytometer was used to count the washed cells after they had been suspended in 20 milliliters of cooled, sterile phosphate buffered saline solution. For each experiment, the blood cell suspension was diluted with phosphate buffered saline solution to 7.068×10^8 cells/mL while being stored on ice. Twenty microliters of peptide were collected and placed in a 2 ml microfuge tube. These tubes were filled with 180 μ l of suspended blood samples, which were then combined. It was determined that the peptide concentration was 250 micro moles per liter. These tubes were then placed in incubation under 37 °C for 40 min. Then these tubes were allowed to cool before being centrifuged for five minutes. A 1.5 ml microfuge tube was filled with 100 μ l of the supernatant. The spectrophotometer was used to measure their absorption²⁷.

Evaluation of Anti-inflammatory activity

User-friendly and economically feasible methods are used to assess the anti-denaturation effects of natural compounds having anti-inflammatory properties. The test apparatus employed 2.5 milliliters of buffered 1% of the total amount of bovine serum albumin (BSA) and 2.5 milliliters of test solution. In order to ensure that the test compounds were dissolved, dimethyl formamide (DMF) was added to the buffer, which was 0.05 M Trisacetate, at a maximum rate of 2.5% (volume/volume). After being heated to 69 °C for four minutes and then cooled, the turbidities of the test and control systems were measured at 660 m μ . A second test was conducted at the same dose for aggregates that reduced turbidity by less than 20% at 1 mM; aggregates that reduced turbidity by more than 20% were considered active and tested at 0.1, 0.2, 0.4, 0.6, and 0.8 mM. 0.1 mM substances that remained active were investigated at even lower concentrations²⁸.

Evaluation of minimum inhibitory concentration (MIC)

The antibacterial activity of extracts derived from the *Perovskia atriplicifolia* Benth has been evaluated using two bacterial strain, *Escherichia coli* and *Staphylococcus aureus*. The liquid culture of these bacteria cultivated in potato dextrose broth yielded the bacterial suspensions. Under standard condition, ELISA plates were developed. Various concentrations of tested samples (20 μ L) were inoculated into the well of ELISA plates. A bacterial suspension having 10 μ L quantity was added in each well of ELISA plates ($OD_{600} = 0.7-0.85$, $\sim 10^8$ CFU/mL). 50 μ L of broth medium was used to dilute the mixtures in the plates. The following dilutions of each tested samples were made: 0, 0.625, 1.5, 2.5, 5, 10, 15, 25, 50, 100, 150, 200, and 250 mg/mL (Figures-9 & 11). Infected micro dilution plates were incubated at 37 °C temperature after covering with para-film. After 24 h, MIC values were calculated from the plates to assess the bacterial growth, and plate photos were then taken²⁷.

Evaluation of Anti-Thrombolytic activity

One milliliter of human blood was placed in centrifuge tubes, and the weighted tubes were then incubated at 35 °C for forty minutes. Following the formation of the clots, the serum was completely removed without causing any damage to the clots, and each tube consisting clots was weighed again to determine the approximate clots weight.

$$\text{Clot weight} = \text{weight of tube including clots} - \text{weight of tube before clot} \quad (1)$$

In different clot-containing tubes, 100 μ l of an aqueous solution of each sample PA, PAH, PAD, PAB, PAE, Fe-NPs and Zn nanoparticles were added. After that, clot lysis was found after all of the tubes were incubated at 37 °C for an hour and thirty minutes. The tubes were weighed again to find out the difference present in weight after clot rupturing, and the discharged fluid was removed following incubation²⁹.

$$\% \text{ clot lysis} = \frac{\text{weight of lysis clots}}{\text{weight of clots before lysis}} \times 100 \quad (2)$$

Statistical analysis

Descriptive statistics were used to summarize the data. The mean and standard error of the mean (SEM) were calculated for each sample ($n=3$) using MS EXCEL. The SEM was determined using the formula $SEM = SD/\sqrt{n}$, where SD is the standard deviation and n is the number of replicates. Due to the small sample size ($n=3$ per treatment), statistical comparisons were not performed, and data interpretation was based on descriptive analysis.

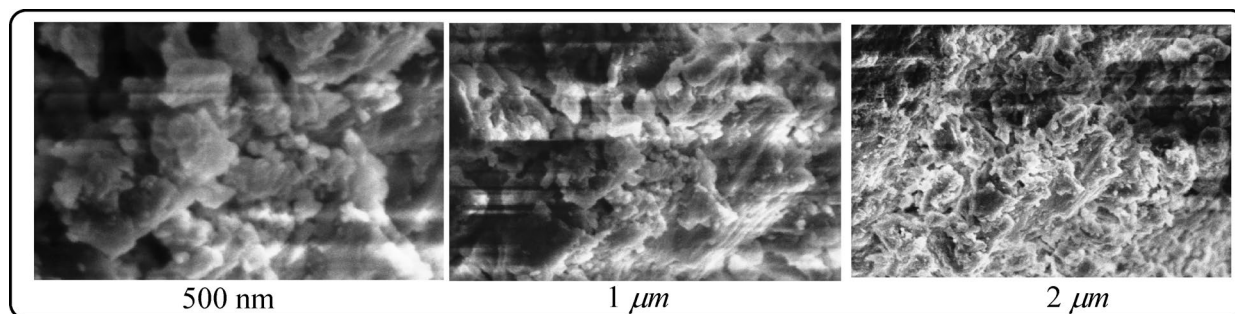


Fig. 1. Scanning electron microscopy (SEM) images of ZnNPs captured at different magnifications: 1 μm , and 2 μm and 500 nm.

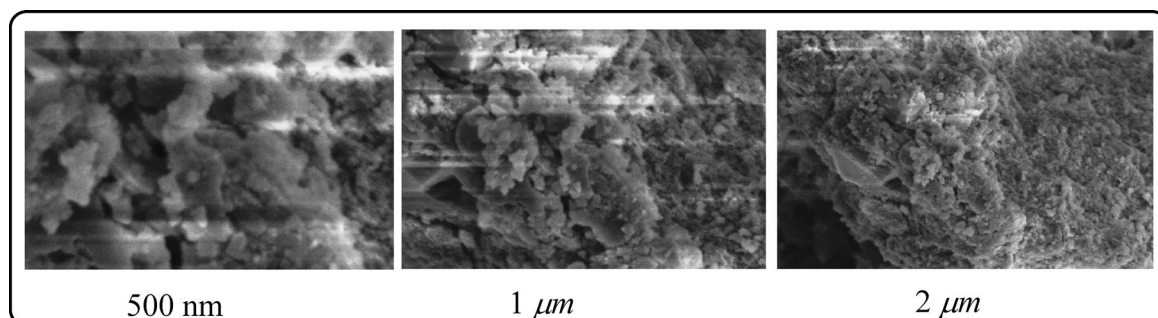


Fig. 2. Scanning electron microscopy (SEM) images of FeNPs captured at different magnifications: 1 μm , and 2 μm and 500 nm.

Additionally, to evaluate the XRD pattern, FT-IR data and UV analysis of green synthesized nanoparticles, correlation analysis was performed on Origin 2021 software.

Results and discussion

SEM analysis of green-synthesize iron and zinc nanoparticles

Figures 1 and 2 show SEM images of zinc and iron nanoparticles, demonstrating effective nanoparticle synthesis. Both particles appear to be nano-sized, with Fe-NPs and Zn-NPs having an average diameter of around 18 nm and 13 nm respectively. Particle adhesion and aggregation during drying could explain whether particles appear irregular and bigger in some regions. However, the irregular aggregation of these particles suggests that the polyphenols and flavonoids were mainly responsible for the capping and reduction of these nanoparticles. Metal reductions in *P. atriplicifolia* extract are induced by a number of naturally occurring chemicals with varying reducing properties. Although pure chemicals produce more thinly spread particles, green synthesized Fe-NPs and Zn-NPs have less aggregates. *P. atriplicifolia* extract contains phytochemicals such as flavonoids, terpenoids, polyphenols, and antioxidants. These chemicals, which function as a capping agent, most likely have a significant impact on nanoparticle aggregation and dispersion³⁰. Because of its high TPC and TFC, *P. atriplicifolia* extract could be a feasible option for producing various metal nanoparticles.

UV-Vis spectroscopy analysis

UV spectroscopy is often used to detect the green synthesized nanoparticles, which focuses on the surface plasmon resonance peaks of subjected formations. Because of the surface plasmon resonance feature, both metals have distinct optical properties. Adding extract at 30–40 °C changed the salt color from greenish to dark brownish green and light orange green, suggesting the synthesis of iron and zinc nanoparticles. These metals were reduced by the active compounds found in the subjected plant, which highlighted with the change in color of solution. These phytochemicals were acted as capping agent for the metal ions. For observing the synthesis of nanoparticles, the stock solution of iron and zinc nanoparticles were prepared in distilled water. Fe and Zn-NPs were shown peaks at 300 and 324 nm, respectively^{31,32} (Figure-3).

X-ray diffraction of iron and zinc nanoparticles

Figures 4 and 5 show XRD patterns for Zn-NPs and Fe-NPs, respectively. It observed that the green synthesized iron and zinc nanoparticles had disorder in character, as few prominent diffraction peaks were present in the whole graph of both nanoparticles. In the case of iron nanoparticles, zero-valent iron observed at a few prominent peaks at 2θ of 37.35°, 45° and 53.6° (Figure-5). At 2θ values of 29.35°, 34.05°, 42.05° and 61.45°, Zn-NPs exhibit less significant results. The broad version of peaks in both patterns at 24°–30° was compatible with

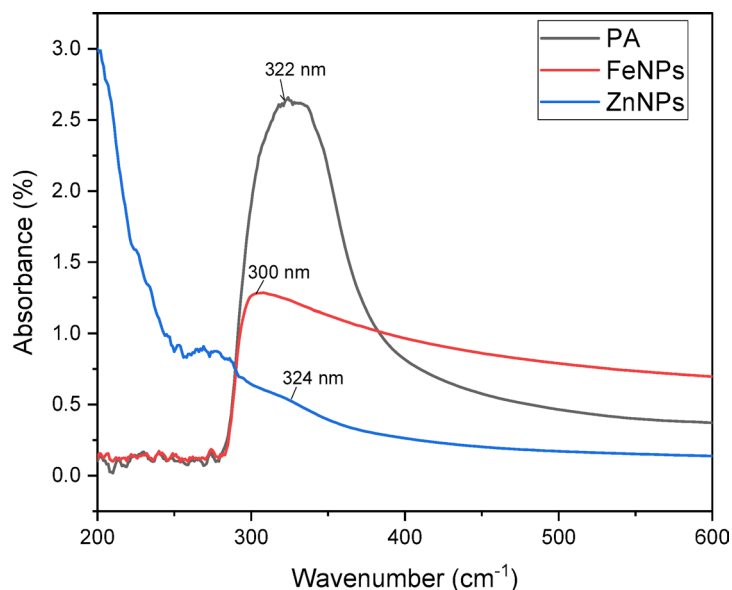


Fig. 3. UV spectra of PA, FeNPs and ZnNPs showing their characteristic absorption peaks.

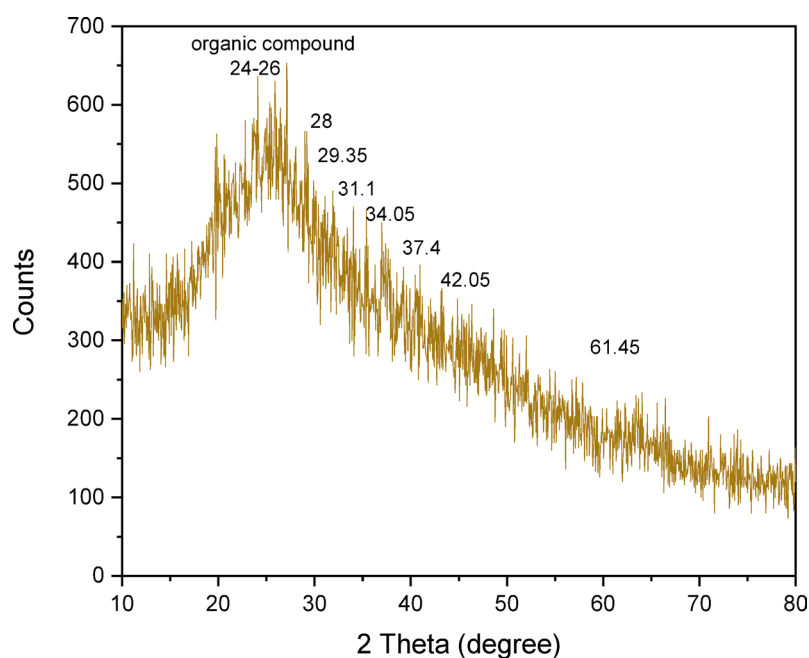


Fig. 4. XRD pattern of the green synthesized Zn-NPs, with the labeled diffraction peaks indicating the characteristic crystalline planes of the Zn nanoparticles.

the following FTIR data, which demonstrated that the phytochemicals were present in *P. atriplicifolia* extract, acted as a stabilizing and capping agent. Previously, *T. chebula* water extract was utilized to produce Fe-NPs, the trend remained consistent³³. This Zn-NPs pattern was linked to a prior study on nanoparticle formation with extracts from *R. sativus* var. Longipinnatus leaves³⁴.

FT-IR analysis

The nature of the crude extract, metal nanoparticles and phytoconstituents of this plant are all determined by the infrared analysis. The stability and shape modification of produced particles are caused by the presence of phytochemicals. A large peak at 3348.27 cm⁻¹ in the crude extract (PA) IR spectra suggested the alcoholic group (perhaps phenolic hydroxyl). The existence of -COOH stretching and -C-H stretching was indicated by signal at 2948.76 cm⁻¹. The existence of C=C in the aromatic and aliphatic areas was indicated by another peak at 1612.24 cm⁻¹. A peak at frequency 1367.93 cm⁻¹ suggested the NO₂ group in the extract. Alkyl halides were

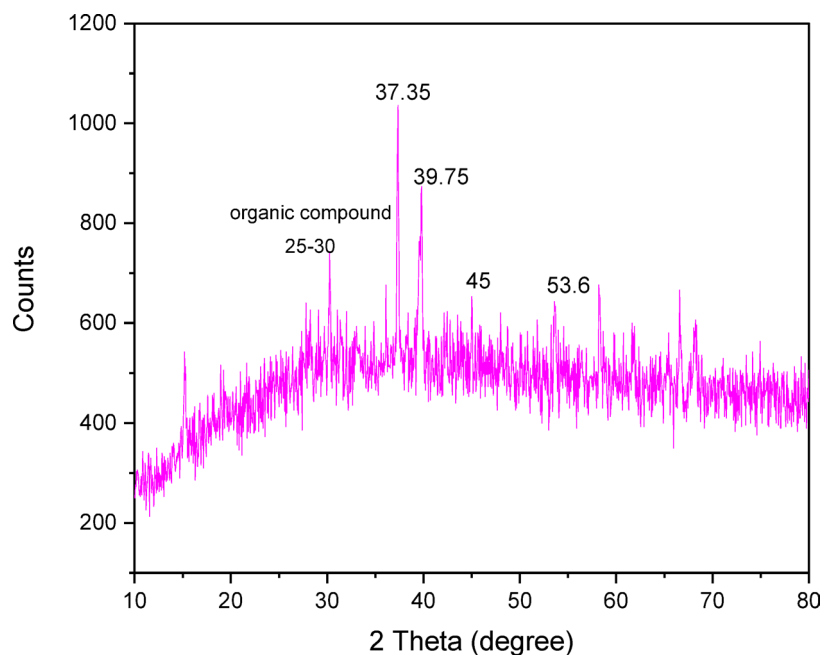


Fig. 5. XRD pattern of the green synthesized Fe-NPs, with the labeled diffraction peaks indicating the characteristic crystalline planes of the Fe nanoparticles.

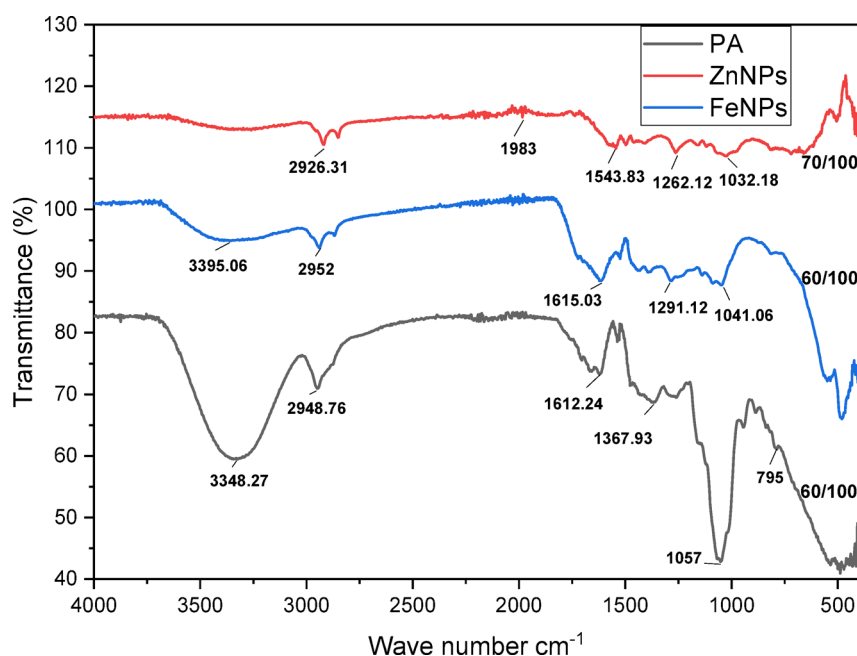


Fig. 6. FT-IR spectra of the crude extract of *P. atriplicifolia*, FeNPs, and ZnNPs, showing shifts in functional group peaks indicative of crude extract involvement in nanoparticle capping.

observed by the peak at frequencies of 1057 and 795 cm^{-1} . The finding of a phenolic -OH group in the sample was demonstrated by the frequency of 3395.06 cm^{-1} in the FT-IR analysis of iron nanoparticles. The C-H bond and -COOH were identified by signal at 2952 cm^{-1} . Additional peaks at frequencies of 1615.03 and 1291.12 cm^{-1} indicate the existence of C=C bond of aromatic and alkene. The presence of alkyl halides is indicated by the transmittance at 1041.06 cm^{-1} . These peaks showed that flavonoids and phenolic components were present. The findings were associated with the green production of FeNPs using eucalyptus leaf extract that had previously been carried out. The existence of -COOH and the C-H bond in ZnNPs FT-IR data is indicated by peak at 2926.31 cm^{-1} . Another peak at 1543.83 cm^{-1} indicates the presence of either C-OH or amide stretching. The alkyl halides in the sample were indicated by the transmittance peak percentage at frequencies of 1262.12

| Phytochemicals | Quantity mean \pm SD | SE |
|-----------------------------------|----------------------------|------|
| Total phenolic components (TPC) | 258.96 \pm 0.56 mg GAE/g | 0.32 |
| Total flavonoids components (TFC) | 511.71 \pm 0.44 mg CE/g | 0.25 |

Table 1. TPC and TFC in the *P. atriplicifolia* crude extract. All experiments were conducted in triplicate, and values are expressed as mean \pm SD (standard deviation), SE (standard error).

| Sr. no. | Sample | Toxicity mean % \pm SD | SE |
|---------|--------------|--------------------------|--------|
| 1 | PAH | 7.45283 \pm 0.0091 | 0.0053 |
| 2 | PAD | 4.90566 \pm 0.0851 | 0.0491 |
| 3 | PAB | 0.943396 \pm 0.011 | 0.0063 |
| 4 | PAE | 0.283019 \pm 0.007 | 0.004 |
| 5 | PAA | 0.943396 \pm 0.0105 | 0.0061 |
| 6 | ZnNPs | 0.09434 \pm 0.0022 | 0.0013 |
| 7 | FeNPs | 1.226415 \pm 0.0065 | 0.0038 |
| 8 | Triton X-100 | 96.415 \pm 0.1993 | 0.115 |
| 9 | PBS buffer | 0 \pm 0.0 | 0 |

Table 2. Cytotoxicity in mean % \pm SD (standard deviation) of the various subjected sample, SE (standard error). All experiments were conducted in triplicate.

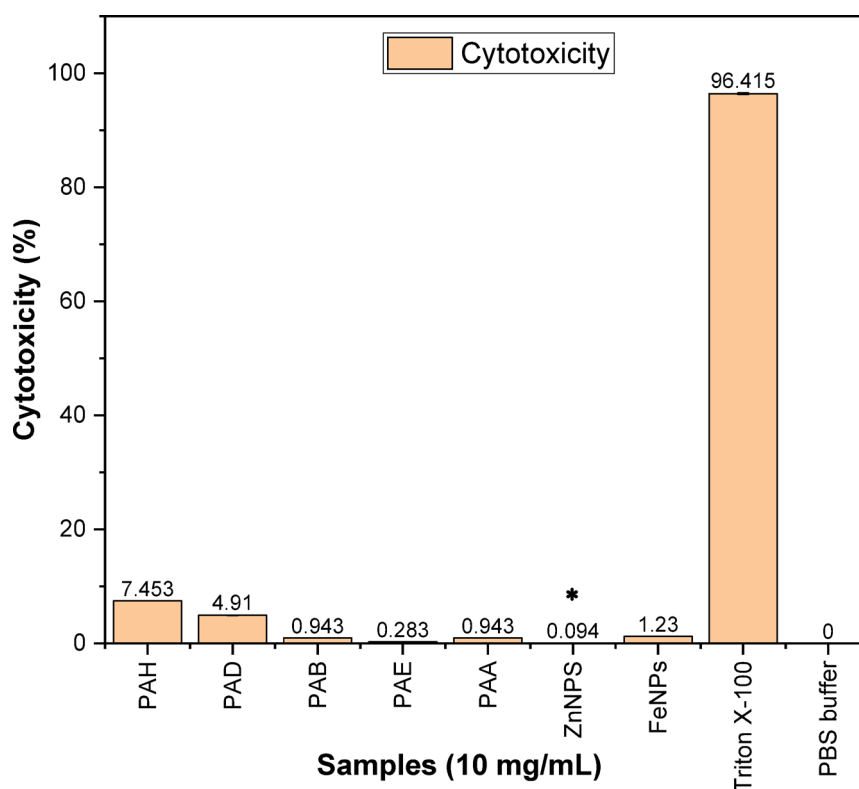


Fig. 7. Cytotoxicity potentials of different fractions of *Perovskia atriplicifolia* and of nanoparticles formed by aqueous solution of its crude extract. (*) potential result.

cm⁻¹ (Figure-6). These findings were linked with the synthesis of zinc nanoparticles using *Cinnamomum verum*, *Brassica oleracea* var. *italica*, *Beta vulgaris* and *C. tamala*. Ultimately, it is determined that these current phytoconstituents which directly contribute to the reduction of iron and zinc metals, were mainly responsible of the formation of nanoparticles^{35–38}.

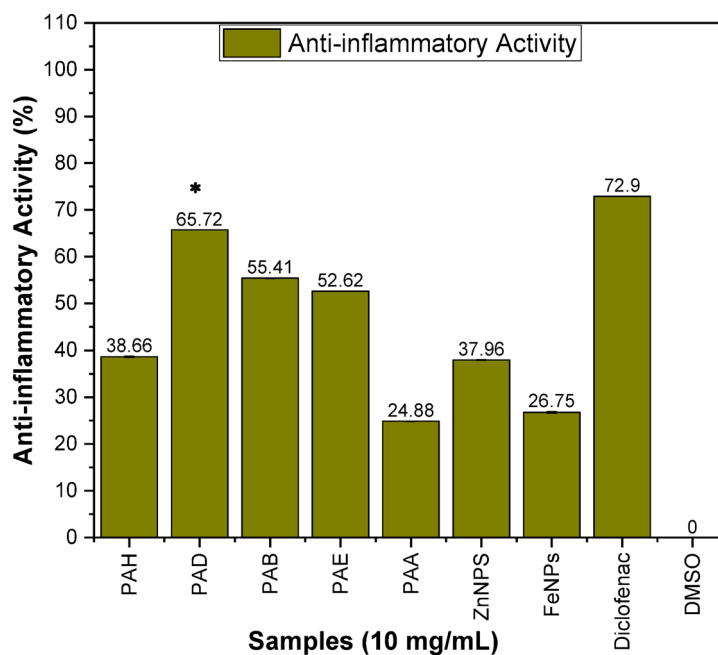


Fig. 8. Anti-inflammatory potentials of different fractions of *Perovskia atriplicifolia* and of nanoparticles formed by aqueous solution of its crude extract, (*) potential result.

| Sr. no. | Sample | Anti-Inflammation Mean % \pm SD | SE |
|---------|------------|-----------------------------------|--------|
| 1 | PAH | 38.66419451 \pm 0.1436 | 0.0829 |
| 2 | PAD | 65.71856741 \pm 0.0056 | 0.0032 |
| 3 | PAB | 55.41390124 \pm 0.0942 | 0.0544 |
| 4 | PAE | 52.62280221 \pm 0.0822 | 0.0475 |
| 5 | PAA | 24.88419555 \pm 0.0778 | 0.0449 |
| 6 | Zn-NPs | 37.95884295 \pm 0.0883 | 0.051 |
| 7 | Fe-NPs | 26.75224595 \pm 0.2126 | 0.1228 |
| 8 | Diclofenac | 72.90 \pm 0.844 | 0.0487 |
| 9 | DMSO | 0.0 \pm 0.0 | 0 |

Table 3. Anti-denaturation activity of tested fractions and green synthesized nanoparticles, SD (standard deviation), SE (standard error). All experiments were conducted in triplicate.

Total phenolic (TPC) and flavonoid components (TFC) in the crude extract

Phytochemicals, which are widely distributed inside the plants and include various phenolic, flavonoid and other beneficial compounds are responsible for the biological potential of many medicinal plants. These substances are important defense mechanisms for plants against environmental threats. For the determination of phenolic and flavonoids components in the *P. atriplicifolia* plant, gallic acid equivalent (mg GAE/g) and catechin (mg CE/g) were used respectively (Table-1).

Cytotoxicity Bio-assay

The toxicity value was evaluated of all the fractions of *P. atriplicifolia* by using hemolytic assay and the Triton X-100 and PBS buffer used as positive and negative control respectively.

Table-2; Figure-7 both showed the toxicity effects of the fractions, made from the crude extract of *Perovskia atriplicifolia* Benth. by using gradient polarity solvents, such as n-hexane, dichloromethane, ethyl acetate, n-butanol and water. The samples were also included with nanoparticles, which prepared by reacting FeCl₃·6H₂O and Zn (CH₃COO)₂ salts with the aqueous solution of crude extract of *Perovskia atriplicifolia*. The toxic impact of these fractions was tested on the healthy human blood cells (RBCs) in the 10 mg/mL concentration. The above results interpret that the nanoparticles of Zn metals showed less toxicity on red blood cells as their values are very close to negative control PBS buffer, i.e. 0.0943 and 3.208 respectively. The PAH and PAD showed high toxicity against red blood cells as their values were 7.4528 and 4.9056 respectively. The cytotoxicity % of PAB and PAA were same i.e. 0.9433 which were shown moderate toxicity towards RBCs because of having toxicities values near to Triton X-100 positive control values which was 96.415.

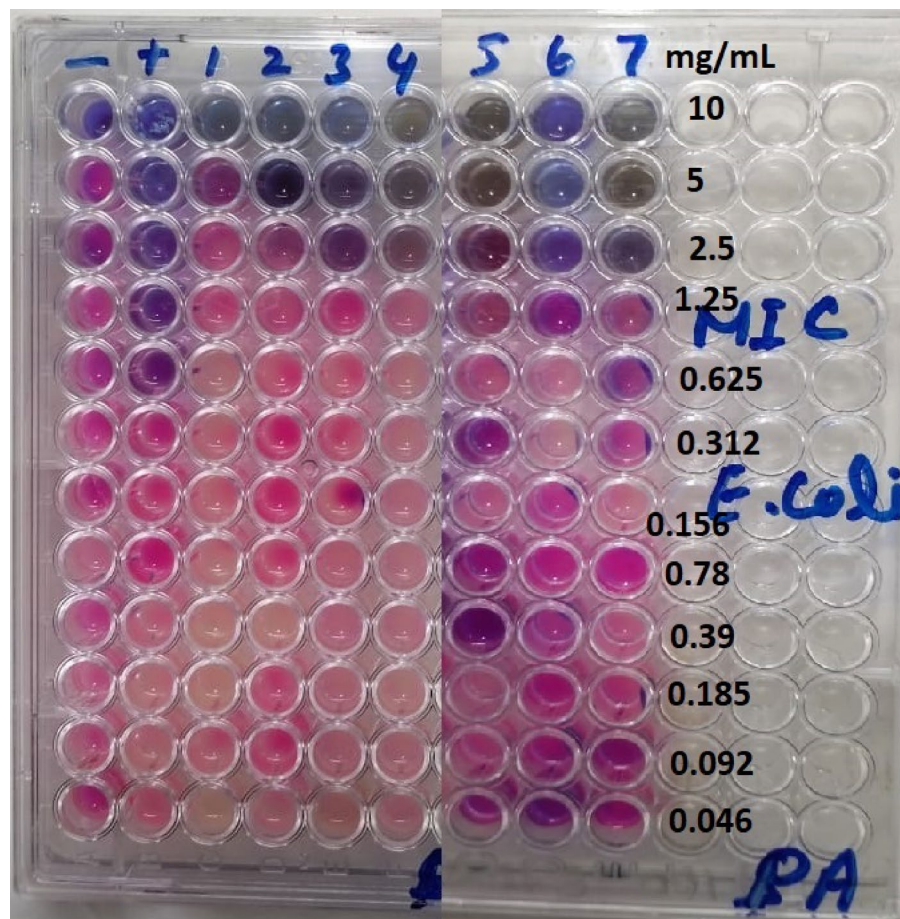


Fig. 9. MIC for the growth inhibition of *E. coli* with different formations of *P. atriplicifolia*. PAH (1), PAD (2), PAB (3), PAE (4), PAA (5), ZnNPs (6), FeNPs (7), Ciprofloxacin (+).

Anti-inflammatory Bio-assay

The anti-inflammation potentials of various fractions of *P. atriplicifolia* have evaluated through BSA (bovine serum albumin) assay. Diclofenac and DMSO used as positive and negative control for this assay respectively (Figure-8).

Table-3; Figure-8 were shown the results of *Perovskia atriplicifolia* Benth. fractions with the nanoparticles which prepared from the aqueous solution of its crude extract. The PAH, PAD, PAB, PAE, PAA showed 38.66%, 65.71%, 55.41%, 52.62% and 24.88% anti-denaturation values which determined that these fractions are active in the inhibition of denaturing of BSA protein. The inhibition percentages of Zn nanoparticles were 37.95% which indicated moderately active behavior of these samples. The nanoparticles of Fe have 26.7522% inhibition value in this assay, which indicated the less activity towards BSA protein than positive control of this assay.

Minimum inhibitory concentration evaluation

The inhibition of bacterial growth was determined by using ELISA plates. These are the sterilized poly styrene plates; in which samples were taken in different concentration to check the minimum required concentration inhibit the growth of bacteria. In this assay, Ciprofloxacin was taken as reference. In the determination of MIC values, two bacterial strains, i.e. *Escherichia coli* and *Staphylococcus aureus* were used.

MIC against *E. coli* The MIC values for *E. coli* were illustrated in Figure-9. In this test, total five fractions and two nanoparticles of Fe and Zn was under examination. The PAH and PAD have 5 mg/ml MIC value. After this, PAB, PAE and PAA have same inhibition capacity, i.e. 2.5 mg/ml. Furthermore, Fe-NPs have 2.5 mg/ml and Zn nanoparticles have 1.25 mg/ml MIC values. The MIC of all these fractions and nanoparticles were expressed in Fig. 10. The Figure-10 was shows the graphical representation of MIC capacity of the five extractions of the *P. atriplicifolia* Benth. and two nanoparticles that was prepared by the reacting the Fe salt and Zn salt with the aqueous solution of the crude extract. Table-4 shows the MIC values of all the fractions and the iron and zinc nanoparticles against *E. coli* strain.

MIC against *S. aureus* In the Figure-11 have shown the MIC of different fractions of *P. atriplicifolia* and nanoparticles upon *Staphylococcus aureus* bacterial strain. Three fractions PAH, PAD, PAB, PAA and iron nanopar-

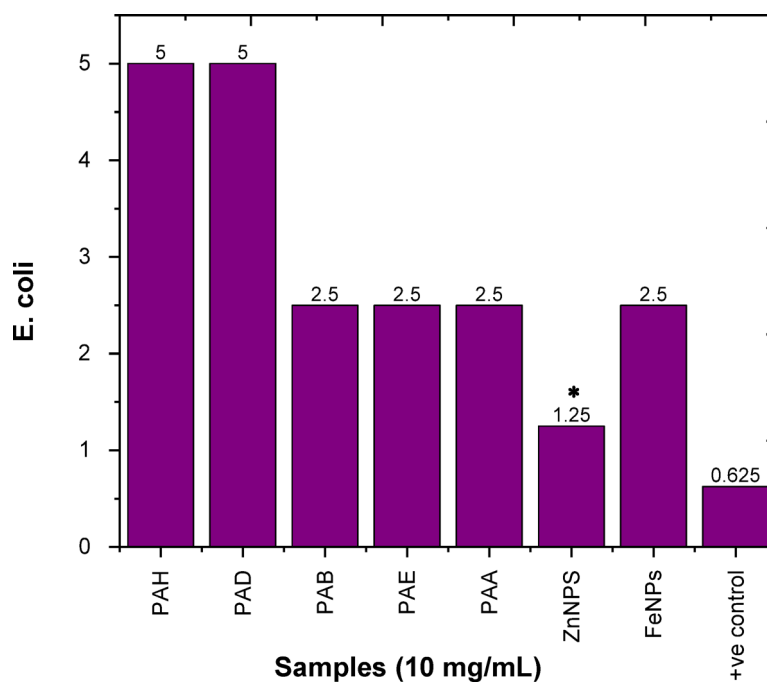


Fig. 10. MIC of the different polarity extracts of *Perovskia atriplicifolia* against *E. coli* bacterial strains. (*) potent result.

| Sample no. | Extraction name | E.coli zone inhibition (mg/ml) |
|------------|-----------------|--------------------------------|
| 1 | PAH | 5 |
| 2 | PAD | 5 |
| 3 | PAB | 2.5 |
| 4 | PAE | 2.5 |
| 5 | PAA | 2.5 |
| 6 | ZnNPs | 1.25 |
| 7 | Fe-NPs | 2.5 |
| 8 | +ve control | 0.625 |

Table 4. MIC values against *Escherichia coli* bacterial strain of various subjected samples.

| Sample no. | Extraction name | S. aureus inhibition (mg/ml) |
|------------|-----------------|------------------------------|
| 1 | PAH | 2.5 |
| 2 | PAD | 2.5 |
| 3 | PAB | 2.5 |
| 4 | PAE | 1.25 |
| 5 | PAA | 2.5 |
| 6 | Zn-NPs | 1.25 |
| 7 | Fe-NP | 0.625 |
| 8 | +ve control | 0.156 |

Table 5. MIC values against *Staphylococcus aureus* bacterial strain of different tested samples.

ticles have equal MIC capacity 0.625 mg/ml against *S. aureus* (Figure-12). Moreover, PAE and zinc nanoparticles have 1.25 mg/ml MIC values. In this method, ciprofloxacin was used as positive control and has MIC 0.156 mg/ml against *E. coli* as shown in Table-5.

The MIC values of the various fractions of *P. atriplicifolia* have indicated that this plant shown great potential in antibacterial activity.

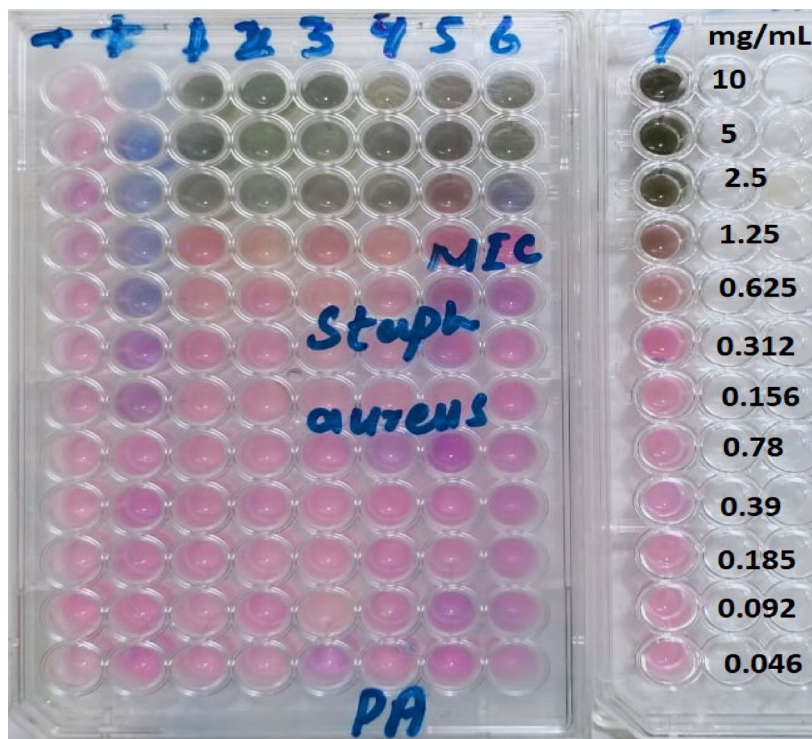


Fig. 11. MIC for the growth inhibition of *S. aureus* with different formations of *P. atriplicifolia*. PAH (1), PAD (2), PAB (3), PAE (4), PAA (5), ZnNPs (6), FeNPs (7), Ciprofloxacin (+).

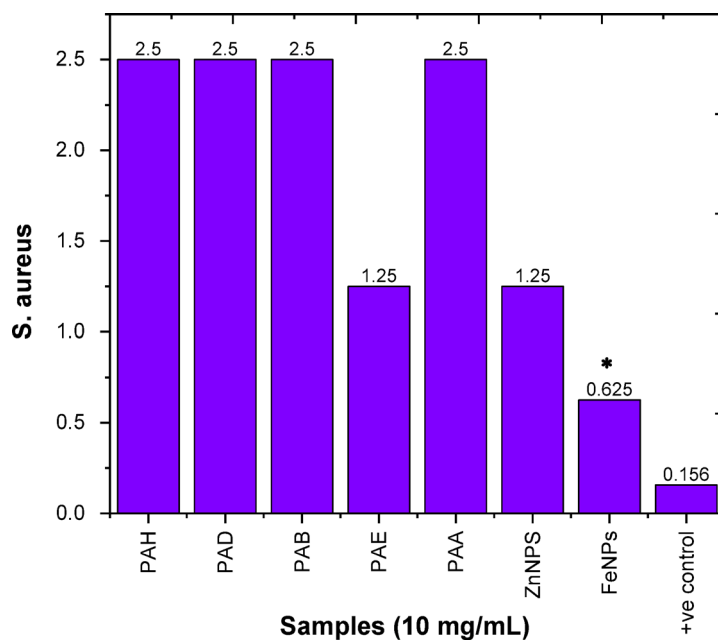


Fig. 12. MIC of the different polarity extracts of *Perovskia atriplicifolia* against *S. aureus* bacterial strains. (*) potential result.

Anti-thrombolytic activity Bio-assay

In Table 6 illustrated the In vitro clot lysis activity of different polarity extracts of *Perovskia atriplicifolia* and the green synthesized nanoparticles. In this assay, clot lysis potential was evaluated against the clots of human blood cells. Streptokinase was used as positive reference and water as negative reference. Following equation was explained the calculation process of clot lysis % in this assay.

| Sr. no. | Sample | Eppendorf weight (g) | Weight of tube and clot(g) | Weight of un-lysis clots (g) | Tube wt. after lysis(g) | Anti-thrombolytic mean % \pm SD | SE |
|---------|---------------|----------------------|----------------------------|------------------------------|-------------------------|-----------------------------------|--------|
| 1 | PAH | 0.71 | 1.99 | 1.28 | 0.21 | 16.40625 \pm 0.0497 | 0.0287 |
| 2 | PAD | 0.71 | 1.99 | 1.28 | -0.607 | 0.421875 \pm 0.0015 | 0.0009 |
| 3 | PAB | 0.71 | 1.99 | 1.28 | 0.23 | 17.96875 \pm 0.0328 | 0.0189 |
| 4 | PAE | 0.71 | 1.99 | 1.28 | 0.27 | 21.09375 \pm 0.0649 | 0.0375 |
| 5 | PAA | 0.71 | 1.99 | 1.28 | 0.25 | 19.53125 \pm 0.0105 | 0.0061 |
| 6 | Zn-NPs | 0.71 | 1.99 | 1.28 | -0.601 | 2.953125 \pm 0.0536 | 0.0309 |
| 7 | Fe-NPs | 0.71 | 1.99 | 1.28 | 0.28 | 21.875 \pm 0.09 | 0.052 |
| 8 | Streptokinase | 0.71 | 1.99 | 1.28 | 1.62 | 71.43 \pm 0.1 | 0.0577 |
| 9 | Water | 0.71 | 1.99 | 1.28 | 0.748 | 2.96 \pm 0.1 | 0.058 |

Table 6. Determination of in vitro anti-thrombolytic % of various extracts, iron and zinc nanoparticles. SD (standard deviation), SE (standard error). All experiments were conducted in triplicate.

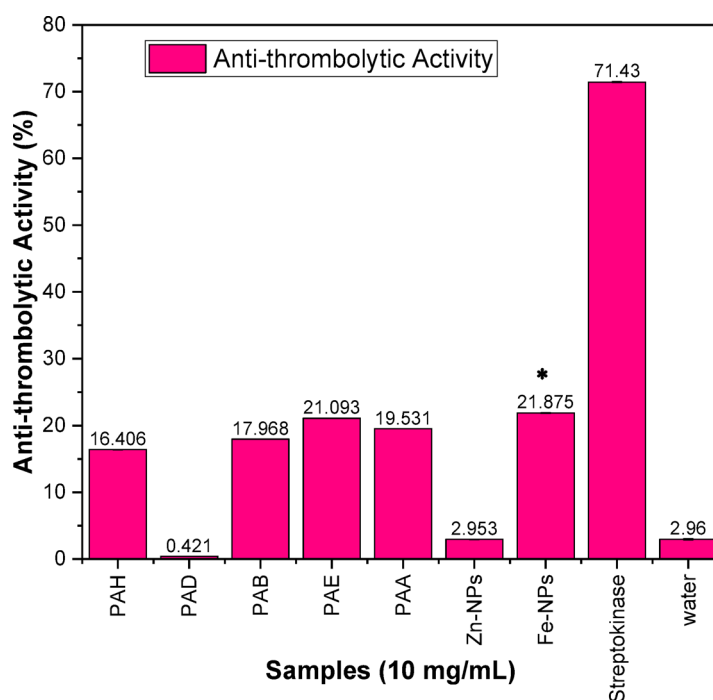


Fig. 13. Anti-thrombolytic activity of various fractions of *Perovskia atriplicifolia* Benth. iron and zinc nanoparticles, (*) potential result.

$$\text{Anti - thrombolytic activity (\%)} = \frac{\text{weight of the lysis clot}}{\text{weight of clot before lysis}} \times 100 \quad (3)$$

Table-6; Figure-13 shows that all the tested formations shown the active potential in clot lysis activity. Streptokinase was used as positive control which has 71.43% clot lysis potential. Water used as negative control which has very minor 2.96% active potential for clot lysis. PAE and PAA have shown great potentials in clot lysis among all the subjected samples which were 21.09375% and 19.53125% respectively. Furthermore, PAB, PAH and PAD fractions have clot lysis potential values 17.96875%, 16.40626%, and 0.421875% respectively. Iron and zinc nanoparticles have anti-thrombolytic values i.e. 21.875% and 2.95312% respectively. Overall all the fractions of *Perovskia atriplicifolia* Benth. have active anti-thrombolytic potentials according to experimental results.

Conclusion

This investigation indicated that the green synthesized nanoparticles have remarkable potentials in biological applications. The successful formation of nanoparticles was observed by the change in color of solutions and by SEM, XRD, FT-IR and UV techniques as well. The Folin-Ciocalteu and aluminum chloride colorimetric assays revealed that this plant have abundance amount of phenolic and flavonoids components which are responsible of its potential in biological activities. Overall, all the extracts of *P. atriplicifolia* showed significant anti-inflammation, anti-bacterial and anti-thrombolytic activities with less toxicities. In case of hemolytic assay, PAE, PAB and Zn-NPs have less toxic effect than other formations i.e. 0.28%, 0.94%, and 0.09% respectively.

30. Pillai, A. M. et al. Green synthesis and characterization of zinc oxide nanoparticles with antibacterial and antifungal activity. *J. Mol. Struct.* **1211**, 128107. <https://doi.org/10.1016/j.molstruc.2020.128107> (2020).
31. Pattanayak, M. & Nayak, P. Green synthesis and characterization of zero valent iron nanoparticles from the leaf extract of *Azadirachta indica* (Neem). *World J. Nano Sci. Technol.* **2**, 06–09. <https://doi.org/10.5829/idosi.wjnst.2013.2.1.21132> (2013).
32. Fakhari, S., Jamzad, M. & Kabiri Fard, H. Green synthesis of zinc oxide nanoparticles: a comparison. *Green. Chem. Lett. Rev.* **12**, 19–24. <https://doi.org/10.1080/17518253.2018.1547925> (2019).
33. Kumar, K. M., Mandal, B. K., Kumar, K. S., Reddy, P. S. & Sreedhar, B. Biobased green method to synthesise palladium and iron nanoparticles using *Terminalia chebula* aqueous extract. *Spectrochim Acta Part. A: Mol. Biomol. Spectrosc.* **102**, 128–133. <https://doi.org/10.1016/j.saa.2012.10.015> (2013).
34. Umamaheswari, A., Prabu, S. L., John, S. A. & Puratchikody, A. Green synthesis of zinc oxide nanoparticles using leaf extracts of *Raphanus sativus* var. Longipinnatus and evaluation of their anticancer property in A549 cell lines. *Biotechnol. Rep.* **29**, e00595. <https://doi.org/10.1016/j.btre.2021.e00595> (2021).
35. Kathyayani, D., Mahesh, B., Gowda, D. C., Sionkowska, A. & Veeranna, S. Investigation of miscibility and physicochemical properties of synthetic polypeptide with collagen blends and their wound healing characteristics. *Int. J. Biol. Macromol.* **246**, 125704. <https://doi.org/10.1016/j.ijbiomac.2023.125704> (2023).
36. Mahesh, B. et al. Interaction between synthetic elastin-like polypeptide and collagen: investigation of miscibility and physicochemical properties. *Polymer* **272**, 125833. <https://doi.org/10.1016/j.polymer.2023.125833> (2023).
37. Hamed, R., Obeid, R. Z. & Abu-Huwaij, R. Plant mediated-green synthesis of zinc oxide nanoparticles: an insight into biomedical applications. *Nanotechnol Rev.* **12**, 20230112. <https://doi.org/10.1515/ntrev-2023-0112> (2023).
38. Verma, N., Kaushal, P. & Sidhu, A. K. Harnessing biological synthesis: zinc oxide nanoparticles for plant biotic stress management. *Front. Chem.* **12**, 1432469. <https://doi.org/10.3389/fchem.2024.1432469> (2024).

Acknowledgements

Muhammad Imran expresses his appreciation to the University Higher Education Fund for funding this research work under Research Support Program for Central labs at King Khalid University through the project number CL/PRI/A/1.

Author contributions

A. H.: Writing, original draft, review and editing; A. B.: Methodology and Investigation; S. A.: review, editing and Writing; M. S. H. A.: Formal analysis, conceptualization. M. I.: writing, review and editing; E. A.: formal analysis and conceptualization; K. K-M.: writing, review and editing; M. G.: supervision and methodology; M. M.: review and editing; M. A.: investigation and conceptualization; M. A. A.: writing, review and editing; K. M.: methodology and investigation; A. J.: review and editing; A. K.: investigation and methodology.

Funding

Muhammad Imran expresses his appreciation to the University Higher Education Fund for funding this research work under Research Support Program for Central labs at King Khalid University through the project number CL/PRI/A/1.

Declarations

Competing interests

The authors declare no competing interests.

Ethical statement

The research described in this manuscript complies with all relevant ethical guidelines and regulations, including those set forth by our institution and any applicable regulatory bodies. We further confirmed that a written informed consent was obtained from our institute's ethical committee namely "Ethical Research Committee, University of Okara" under the Ethics Approval Number # ERC/UO/250E prior conducting this research. All human participants involved in this study provided informed consent prior to their inclusion. We have taken measures to ensure that participants fully understood the nature of the research, their rights, and the potential risks and benefits involved. Any identifying information pertaining to participants has been anonymized to protect their privacy. All procedures involving humans and other biological samples were performed with care and consideration for their welfare, and efforts were made to minimize pain, distress, and suffering.

Additional information

Correspondence and requests for materials should be addressed to A.H.

Reprints and permissions information is available at www.nature.com/reprints.

Publisher's note Springer Nature remains neutral with regard to jurisdictional claims in published maps and institutional affiliations.

Open Access This article is licensed under a Creative Commons Attribution-NonCommercial-NoDerivatives 4.0 International License, which permits any non-commercial use, sharing, distribution and reproduction in any medium or format, as long as you give appropriate credit to the original author(s) and the source, provide a link to the Creative Commons licence, and indicate if you modified the licensed material. You do not have permission under this licence to share adapted material derived from this article or parts of it. The images or other third party material in this article are included in the article's Creative Commons licence, unless indicated otherwise in a credit line to the material. If material is not included in the article's Creative Commons licence and your intended use is not permitted by statutory regulation or exceeds the permitted use, you will need to obtain permission directly from the copyright holder. To view a copy of this licence, visit <http://creativecommons.org/licenses/by-nc-nd/4.0/>.

© The Author(s) 2025